# Machine LearningDriven Identification of Factors Governing Secondary Organic Aerosol Formation During Autumn in Beijing

**Liu, Jun; Wang, Yonghong; Chu, Biwu; Zhang, Chunyan; Huang, Wei ...**

**2025-12-28**

John Wiley and Sons Inc.

http://hdl.handle.net/10138/625781

Liu, J, Wang, Y, Chu, B, Zhang, C, Huang, W, Liu, Q, Li, S, Liu, Y, Chen, T, Li, H, Zhang, P, Ma, Q, Mu, Y, Jiang, J, Wang, S, He, K, Worsnop, D R & He, H 2025, 'Machine LearningDriven Identification of Factors Governing Secondary Organic Aerosol Formation During Autumn in Beijing', Geophysical Research Letters, vol. 52, no. 24, e2025GL119745. https://doi.org/10.1029/2025gl119745

Geophysical Research Letters

RESEARCH LETTER
10.1029/2025GL119745

# Machine Learning-Driven Identification of Factors Governing Secondary Organic Aerosol Formation During Autumn in Beijing

**Jun Liu[1,2], Yonghong Wang[1,2], Biwu Chu[1,2,3], Chunyan Zhang[1,2], Wei Huang[4], Quan Liu[5], Shuying Li[1,2], Yuan Liu[6], Tianzeng Chen[1,2], Hao Li[1,2], Peng Zhang[1,2], Qingxin Ma[1,2,3], Yujing Mu[1,2], Jingkun Jiang[7,8], Shuxiao Wang[7,8], Kebin He[7,8], Douglas R. Worsnop[9,10], and Hong He[1,2,11]**

[1]Laboratory of Atmospheric Environment and Pollution Control, Research Center for Eco-Environmental Sciences, Chinese Academy of Sciences, Beijing, China, [2]University of Chinese Academy of Sciences, Beijing, China, [3]State Key Laboratory of Regional Environment and Sustainability, Research Center for Eco-Environmental Sciences, Chinese Academy of Sciences, Beijing, China, [4]School of Environmental and Municipal Engineering, Xi'an University of Architecture and Technology, Xi'an, China, [5]State Key Laboratory of Severe Weather & Key Laboratory of Atmospheric Chemistry of CMA, Chinese Academy of Meteorological Sciences, Beijing, China, [6]Washington University in St. Louis, St. Louis, MO, USA, [7]State Key Laboratory of Regional Environment and Sustainability, School of Environment, Tsinghua University, Beijing, China, [8]Key Laboratory of Sources and Control of Air Pollution Complex, Ministry of Ecology and Environment, Beijing, China, [9]Institute for Atmospheric and Earth System Research / Physics, Faculty of Science, University of Helsinki, Helsinki, Finland, [10]Aerodyne Research, Inc., Billerica, MA, USA, [11]State Key Laboratory of Advanced Environmental Technology, Institute of Urban, Environment, Xiamen, China

**Key Points:**

- Interpretable machine learning successfully identifies key factors governing secondary organic aerosol (SOA) formation
- Aerosol liquid water content governs aqueous SOA formation
- Particulate organic nitrate production is constrained more by gas-particle partitioning

**Supporting Information:**

Supporting Information may be found in the online version of this article.

**Correspondence to:**

Y. Wang and B. Chu,
yonghongwang@rcees.ac.cn;
bwchu@rcees.ac.cn

**Citation:**

Liu, J., Wang, Y., Chu, B., Zhang, C., Huang, W., Liu, Q., et al. (2025). Machine learning-driven identification of factors governing secondary organic aerosol formation during autumn in Beijing. *Geophysical Research Letters*, *52*, e2025GL119745. https://doi.org/10.1029/2025GL119745

Received 29 SEP 2025
Accepted 1 DEC 2025

**Abstract** Organic aerosol (OA) and its constituent particulate organic nitrate (pON) are critical factors affecting air quality and climate, yet their sources and transformation processes remain poorly understood. Machine learning (ML) excels at identifying nonlinear relationships among features, and in this study, interpretable ML is employed to identify the key factors governing OA and pON formation during an autumn field campaign in Beijing. Results demonstrate that both aerosol liquid water content (ALWC) and aerosol surface area are two primary factors governing the formation of OA and pON. Specifically, OA formation was predominantly driven by ALWC that is associated with aqueous-phase processes or gas-liquid partitioning, particularly during severe pollution episodes. pON formation was constrained by aerosol surface area, indicating the vital contribution of gas-to-particle partitioning from low volatility vapors or interface processes of precursors. Our results provide new insights into OA formation mechanisms.

**Plain Language Summary** Organic aerosol (OA) and particulate organic nitrate (pON) represent significant components of atmospheric particulate matter. Current understanding of their formation mechanisms remains inadequate, particularly regarding the contributions from different formation pathways. This knowledge gap constitutes a significant source of uncertainty in numerical modeling and impedes accurate assessment of their environmental and climate impacts. In this study, we propose an explainable machine learning (ML) approach to quantitatively assess the effects and relative importance of different pathways on the formation of OA and pON. Aerosol liquid water content (ALWC) and aerosol surface area (Sa) were identified as the two most critical factors influencing the formation of OA and pON. They can be regarded as representative variables for aqueous-phase and gas-phase processes, respectively. Notably, OA formation is primarily controlled by ALWC, suggesting aqueous-phase processes likely dominate its production. Conversely, pON formation is mainly regulated by Sa, indicating greater influence from gas-phase processes or equilibrium partitioning of soluble organic vapors. Compared to numerical models, the ML-based approach provides a flexible tool for rapidly assessing the relative importance of different physicochemical processes without relying on explicit chemical mechanisms.



## 1. Introduction

Secondary organic aerosol (SOA) constitutes the dominant fraction of OA on a global scale (Jimenez et al., 2009). However, incomplete understanding of its complex formation mechanisms introduces substantial uncertainties in numerical model simulations, impeding accurate assessment of its global significance (Hallquist et al., 2009; R. J.

Huang et al., 2025). The conventional paradigm holds that SOA formation primarily originates from gas-particle partitioning (GPP) of less-volatile intermediates produced through gas-phase oxidation of volatile organic compounds (VOCs) (Odum et al., 1996; Shiraiwa & Seinfeld, 2012), which has been widely regarded as the main formation pathway of SOA on a global scale (Hallquist et al., 2009; Jimenez et al., 2009). Meanwhile, a growing body of modeling and experimental evidence demonstrates that aqueous-phase chemical reactions in clouds and wet aerosols also represent a significant pathway for SOA formation (Ervens et al., 2011; Lim et al., 2010). SOA generated through these two distinct pathways is termed gasSOA (gas-phase-originated SOA) and aqSOA (aqueous-phase-formed SOA), respectively (Ervens et al., 2011; Kuang et al., 2020). Clarifying the dominant pathways of SOA formation across different regions is essential for understanding their associated environmental and climatic impacts, as well as for developing targeted control strategies.

The oxidation of precursor VOCs generates intermediate products with varying volatility distributions, where lower-volatility components exhibit a higher tendency to be distributed in the particulate phase (Donahue et al., 2006; Odum et al., 1996). Traditionally, functionalization and oligomerization reactions have been considered the dominant pathway for SOA formation (Denkenberger et al., 2007; Gao et al., 2004). Recent studies suggest that intense production of SOA via GPP of low-volatility oxygenated organic molecules generated via autoxidation pathways contributes to haze formation (Nie et al., 2022; Y. H. Wang et al., 2022; C. Yang et al., 2023). These gas-phase reaction pathways are influenced by multiple environmental factors, such as temperature (Odum et al., 1996), relative humidity (RH) (Jia & Xu, 2014; Sarrafzadeh et al., 2016), oxidant concentrations (T. Z. Chen et al., 2023; McFiggans et al., 2019), $NO_x$ levels (Sarrafzadeh et al., 2016; L. Xu et al., 2014), which collectively determine the characteristics of oxidation products. Interface properties also play a crucial role in GPP processes. For instance, the partitioning may be limited by available aerosol surface area (Sa) for condensation (McVay et al., 2014; Pankow & Bidleman, 1992). The viscosity, phase state, and surface polarity of aerosols affect SOA formation by modulating molecular diffusion and adsorption processes (DeRieux et al., 2018; Song et al., 2016). The presence of inorganic sulfate and nitrate in aerosols significantly enhances hygroscopicity, thereby increasing aerosol liquid water content (ALWC) and promoting aqueous-phase reactions (Wu et al., 2018; Xie et al., 2020). Existing research in the North China Plain demonstrates that gasSOA dominates when photochemical activity is high (Duan et al., 2020; Kuang et al., 2020; W. Q. Xu et al., 2017; Y. Zheng et al., 2021). However, during haze events, elevated ALWC substantially enhances aqueous-phase processes (W. Q. Xu et al., 2017; Y. Zheng et al., 2021), with aqSOA potentially contributing over 50% of total SOA mass concentrations under severe haze conditions (Sapkota et al., 2025).

Particulate organic nitrate (pON) is a significant contributor to the OA mass and serves as a temporary reservoir for $NO_x$, thereby influencing reactive nitrogen chemistry in the atmosphere (Lin et al., 2021; Ng et al., 2017; L. Xu et al., 2015). The formation pathway of pON is complex and not yet fully understood. The prevailing view suggests that GPP of gaseous ON is the dominant pathway, with them being generated through $NO_x$-involved photooxidation of VOCs during daytime and nocturnal $NO_3$ radical oxidation of VOCs (Ng et al., 2017). Some studies suggest that aqueous-phase processes also play an important role (W. Huang et al., 2021; Zare et al., 2018). Recent research also revealed that heterogeneous reactions between organic peroxides and nitrite are a key source of pON (Y. Yang et al., 2025). Therefore, evaluating the formation mechanisms of pON can help us better understand their role in the formation and evolution of particulate pollution.

Current field studies evaluate the relative contributions of gasSOA and aqSOA primarily through source apportionment based on SOA composition (D. D. Huang et al., 2018), while it is difficult to identify the key factors governing their formation pathways. Machine learning (ML) techniques have gained widespread application in atmospheric chemistry research owing to their capacity to capture complex nonlinear relationships and provide quantitative feature importance metrics (Hou et al., 2022). Most ML algorithms exhibit strong, excellent predictive performance, yet they typically function as "black box" models, lacking intrinsic interpretability. Currently, the Shapley Additive exPlanations (SHAP) method (Lundberg & Lee, 2017; Lundberg et al., 2020), grounded in game theory, enables quantitative assessment of feature contributions, thereby facilitating interpretable analysis of ML model results.

An autumn field campaign was employed to investigate SOA and pON formation. By applying an ML framework, we aimed to identify and quantify key factors of their formation, providing mechanistic insights into potential formation pathways.

## 2. Materials and Methods

### 2.1. Field Campaign and Instruments

The field observation was performed at a typical urban site in Beijing from 1 October to 12 November 2021 on the rooftop (8th floor) of Building 5 at the Research Center for Eco-Environmental Sciences, Chinese Academy of Sciences (RCEES, CAS; 40.02°N, 116.35°E) situated in the Haidian District. This site is surrounded primarily by office and residential buildings, with road traffic and domestic emissions serving as the dominant pollution sources, making it representative of typical urban environments (Xuan et al., 2024; Zhang et al., 2024; X. Zhao et al., 2025).

Non-refractory submicron aerosol components (NR-$PM_1$: OA, nitrate, sulfate, ammonium, chloride) were measured in real time by a high-resolution time-of-flight aerosol mass spectrometer (HR-ToF-AMS), with detailed measurement and calibration information described in a previously published paper (T. Z. Chen et al., 2020; Zhang et al., 2024). The concentration and mixing state of black carbon (BC) were measured in real time by a single particle soot photometer (SP2, Droplet Measurement Technologies, Boulder, CO). The aerosol surface area concentration (Sa) was derived from the particle size distribution measured by two scanning mobility particle sizers (DMA 3081A with CPC 3775 and DMA 3085 with CPC 3776, TSI). Gaseous species were measured as follows: nitrogen oxides ($NO_x$) by Thermo 42i-TL, sulfur dioxide ($SO_2$) by Thermo 43i, carbon monoxide (CO) by Thermo 48i, ozone ($O_3$) by Thermo 49i, ammonia ($NH_3$) by Aerodyne QC-TILDAS, and formaldehyde (HCHO) by Picarro G2307. Signals of Nitric acid ($HNO_3$) and nitryl chloride ($ClNO_2$) were measured by a chemical ionization time-of-flight mass spectrometer coupled with an iodide chemical ionization source (ToF-CIMS, Aerodyne Research, Inc. USA). The calibration of $HNO_3$ was performed through $HNO_3$ permeation tubes (Valco Instrument Company Inc. Metronics) with a permeation rate of 44 ng $min^{-1}$ at 30°C, and the normalized signal of $ClNO_2$ was used in the analysis.

Gaseous nitrous acid (HONO) was measured in real time by a water-based long-path absorption photometer (WLPAP, Beijing Zhicheng Technology Co.). Meteorological parameters (temperature T, relative humidity RH, wind speed WS, and wind direction WD) were simultaneously observed by a meteorological station (Vaisala). Ultraviolet radiation (UV, 290–400 nm) data were collected by a CUV3 broadband UV radiometer from Kipp & Zonen (Netherlands).

### 2.2. Aerosol Liquid Water Content (ALWC) and Acidity

The estimated ALWC arises from the combined contribution of water associated with both inorganic ($W_i$) and organic components ($W_o$). Here, $W_i$ was derived from the ISORROPIA-II thermodynamic equilibrium model in forward mode, where $W_o$ was calculated based on the $\kappa$-Köhler theory (Lambe et al., 2011). The ALWC in this study has been previously reported (Zhang et al., 2024). Besides, aerosol pH was calculated by considering $H_{air}^+$ and the total ALWC (Guo et al., 2015). Detailed calculation procedures and technical specifics have been described in the previous report (W. Huang et al., 2021).

### 2.3. Estimation of Particulate Organic Nitrate

Particulate organic nitrate (pON) concentrations were quantified using the $NO_2^+/NO^+$ fragment ratio method derived from the HR-ToF-AMS measurements. This approach exploits the distinct $NO_2^+/NO^+$ fragmentation patterns between organic and inorganic nitrates (Day et al., 2022; Farmer et al., 2010; Fry et al., 2013; L. Xu et al., 2015), a well-validated methodology widely applied in field observations of pON. Specifically, inorganic nitrate exhibits a characteristic $NO_2^+/NO^+$ ratio ($R_{AN}$) of approximately 0.4, while the ratio for pON ($R_{ON}$) varies between 0.08 and 0.2 (Boyd et al., 2015), depending on the specific pON composition. The selection of $NO_2^+/NO^+$ ratios for pON quantification introduces uncertainties due to: (a) compositional dependence of the fragmentation pattern and (b) potential inter-instrument variability. During our field campaign, the $R_{ON}$ was set to 0.1, which also represents the lowest value observed in this study (Zhang et al., 2024). The selection of the $R_{ON}$ value introduces the main uncertainty in pON calculations. However, it is noteworthy that the influence of the $R_{ON}$ value on pON concentrations is linear, which has no significant impact on the results of ML models.

### 2.4. Description of Machine Learning Methods

To identify the optimal ML model for this study, we evaluated the performance of several commonly used algorithms including Linear Regression (LR), Light Gradient Boosting Machine (LightGBM), eXtreme Gradient Boosting (XGBoost), and Random Forest (RF) in predicting OA and pON. The models were trained on hourly data ($N = 843$), with the data set randomly partitioned into 70% for training and 30% for independent tests (Text S1 in Supporting Information S1). We found that employing stratified sampling for data set splitting yields more stably distributed independent validation sets compared to the default simple random sampling method (Figure S2 in Supporting Information S1). Model training incorporated 5-fold cross-validation and learning curve-based hyperparameter optimization. The models' final performance was assessed using the coefficient of determination ($R^2$), mean absolute error, and root mean square error (RMSE) on the independent validation set (Text S1.3 in Supporting Information S1). The choice of random seeds during data set splitting also significantly affects model performance (Figure S3 in Supporting Information S1). To mitigate this effect, we averaged the results obtained from 50 different random seeds (Figure S6 in Supporting Information S1). The results demonstrate that LightGBM, XGBoost, and RF performed comparably well ($R^2 \approx 0.95$ and RMSE $\approx 1.4$ μg m$^{-3}$ for OA, $R^2 \approx 0.86$ and RMSE $\approx 0.31$ μg m$^{-3}$ for pON) and significantly outperformed LR ($R^2 = 0.92$ and RMSE = 1.8 μg m$^{-3}$ for OA, $R^2 = 0.67$ and RMSE = 0.47 μg m$^{-3}$ for pON). We ultimately selected RF for subsequent computations in this study.

Model interpretability was achieved through SHAP, a game theory-based approach (see Supporting Information S1 for details). It should be noted that when applying SHAP analysis, interdependencies among features may lead to additive contributions, potentially affecting quantitative interpretations of individual feature importance. Furthermore, different random seeds also lead to variations in feature importance rankings (Figures S4 and S5 in Supporting Information S1). We determined the random seeds for the prediction models of OA and pON based on the average results of feature importance rankings across 50 random seeds.

## 3. Results

### 3.1. Overview of Autumn Field Observation

Figure 1 presents the temporal variations of NR-$PM_1$ composition, gaseous precursors, and meteorological parameters during the field campaign. We categorized the data into three intervals based on $PM_1$ concentrations, representing the clean period ($PM_1 \leq 5$ μg m$^{-3}$, $N = 434$ hr), medium aerosol loading period (5 μg m$^{-3}$ < $PM_1$ < 30 μg m$^{-3}$, $N = 374$ hr), and high aerosol loading period ($PM_1 \geq 30$ μg m$^{-3}$, $N = 268$ hr). NR-$PM_1$ was predominantly composed of organic aerosol (OA) and nitrate, with nitrate emerging as the major secondary inorganic component. Throughout the observation period, OA concentrations ranged from 0.6 to 24.8 μg m$^{-3}$ (mean: 6.6 μg m$^{-3}$), accounting for 22%–90% of NR-$PM_1$ (mean: 50%). OA exhibited higher fractional contributions during clean periods, while nitrate became dominant during more polluted episodes (Figure S8 in Supporting Information S1). Nitrate concentrations averaged 7.1 μg m$^{-3}$, representing 24% of NR-$PM_1$ on average (peaking at 54%). pON displayed concentration trends consistent with pollution levels, averaging 0.8 μg m$^{-3}$ (maximum: 5.1 μg m$^{-3}$) and contributing 10%–42% to OA mass, with proportionally higher contributions during medium aerosol loading.

Two precipitation events occurred during the observation period (Figure 1): (a) a 9-hr rainfall starting at 16:00 on 3 October and (b) a 20-hr snowfall beginning at 11:00 on 6 November. Before the rainfall, gradual accumulation of pollution precursors increased particulate matter concentrations, which in turn diminished solar radiation, and elevated ALWC (53.7 ± 49.0 μg m$^{-3}$, peaking at 219.4 μg m$^{-3}$)—conditions conducive to aqueous-phase reactions. In contrast, pre-snowfall conditions exhibited sustained RH > 50% for approximately 4 days, with ALWC reaching significantly higher levels (maximum: 583 μg m$^{-3}$) compared to the pre-rainfall period. Notably, lower $O_x$ (=$NO_2$ + $O_3$) concentrations before snowfall created more favorable conditions for photochemical reactions than those preceding rainfall.

### 3.2. Factors Controlling SOA Formation

The SHAP method was employed to evaluate the RF model outputs, quantifying the contribution of individual variables to ambient OA and pON formation during the field campaign illustrated in Figures 2 and 3, respectively. The mean absolute SHAP value across all samples represents a variable's global-scale importance or contribution

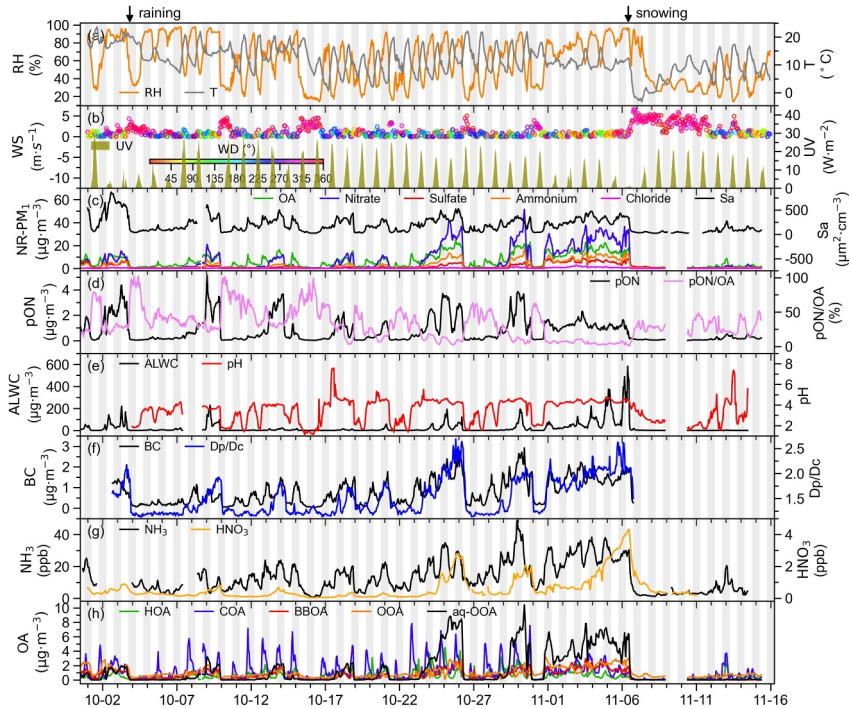


**Figure 1.** Time series of pollutant concentrations during this field observation: (a) temperature (T) and relative humidity, (b) wind speed/direction (WS/WD) and solar radiation (UV), (c) NR-$PM_1$ composition and concentration, (d) particulate organic nitrates (pON) and pON/Organic aerosol (OA) ratio, (e) aerosol liquid water content and acidity (pH), (f) black carbon concentration and shell-core diameter ratio (Dp/Dc), (g) ammonia ($NH_3$) and gaseous nitric acid concentrations ($HNO_3$), and (h) positive matrix factorization-resolved OA components. The gray shading represents the nighttime period from 18:00 to 06:00 the following day. The rain lasted for 9 hr, while the snow persisted for 20 hr.

to OA formation throughout the study period. The direction of this contribution (positive or negative influence) is determined by the SHAP value's sign (Figures 2b and 3b). A positive correlation between SHAP values and feature values (variable magnitudes) indicates a positive contribution, whereas a negative correlation reflects an inhibitory effect. For instance, the positive SHAP values of ALWC consistently corresponded to higher ALWC values, demonstrating that elevated aerosol liquid water promotes OA formation.

ALWC, aerosol surface area (Sa), CO, $NH_3$, and $HNO_3$ are the five most influential factors governing OA concentration, which are mechanistically linked to aqueous-phase reaction (ALWC), available surfaces for gas-phase precursors or oxidation product condensation (Sa), primary emission (CO), and aerosol acidity ($NH_3$ and $HNO_3$), respectively. All these five factors demonstrate a monotonically increasing promotion effect on OA concentration enhancement (Figures 2c–2f and Figure S10 in Supporting Information S1). Notably, ALWC was identified as the most important factor (~25%), highlighting the crucial role of aqueous-phase processes or gas-liquid partitioning in SOA formation. ALWC increases significantly as aerosol loading increases, especially under high aerosol loading, where ALWC can even exceed the $PM_1$ concentration. The partial dependence analysis (Figure 2c) demonstrates a monotonic increase in SHAP values of about 4.5 μg $m^{-3}$ (from −2.0 to 2.5) as ALWC rises from less than 1 μg $m^{-3}$ to more than 100 μg $m^{-3}$ during the observation period, suggesting its contribution to aqSOA formation. Given that the observed OA concentration increases from 2.5 to 16.9 μg $m^{-3}$, this ALWC increase potentially accounts for approximately 31% of the observed OA enhancement. The abrupt change in SHAP values with increasing ALWC likely reflects a phase state transition in aerosols, where enhanced aqueous conditions promote SOA formation through accelerated aqueous-phase chemistry and improved mass transfer of precursor gases into the particle phase (Ervens et al., 2011). The ALWC levels in Beijing consistently exceed those observed in other major cities worldwide (Nguyen et al., 2016; Rogers et al., 2025), attributable primarily to higher concentrations of hygroscopic secondary inorganic aerosols coupled with elevated RH during pollution episodes (Duan et al., 2024; Xie et al., 2020).

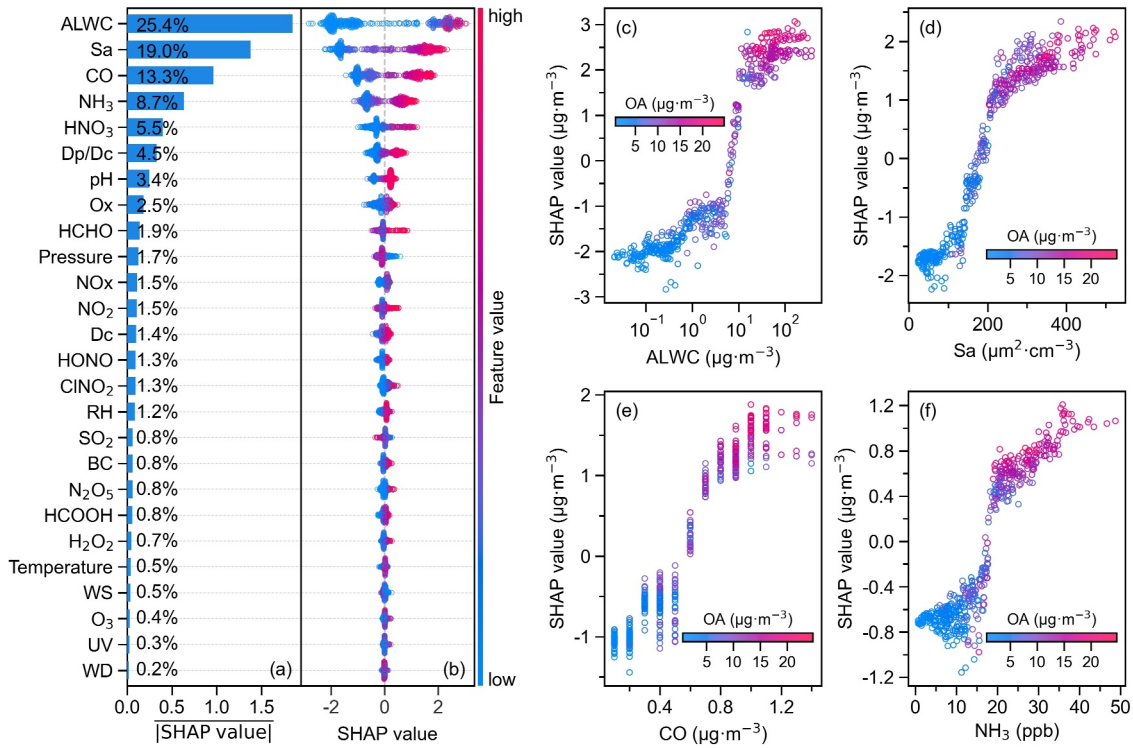


**Figure 2.** (a) Interpreting feature importance rankings from random forest models with organic aerosol (OA) as the dependent variable using Shapley Additive exPlanations analysis. (b) Beeswarm plots of individual feature contributions. (c–f) Dependence plot for the top 4 features.

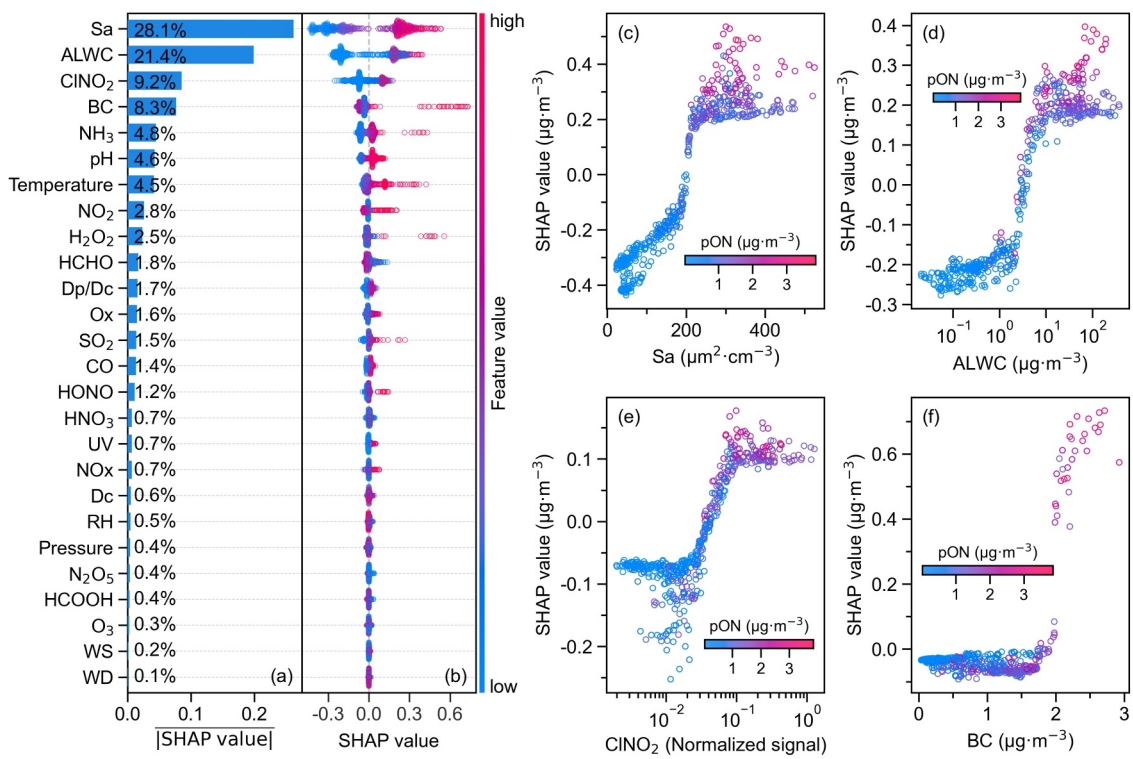


**Figure 3.** (a) Interpreting feature importance rankings from random forest models with particulate organic nitrate (pON) as the dependent variable using Shapley Additive exPlanations analysis. (b) Beeswarm plots of individual feature contributions. (c–f) Dependence plot for the top 4 features.

To quantitatively assess the contribution of aqSOA to total OA and concurrently validate the reliability of the ML approach, positive matrix factorization (PMF) analysis was conducted, as detailed in our previous publication based on the same field campaign (Zhang et al., 2024). The PMF resolved OA into three primary OA (POA) factors (hydrocarbon-like OA [HOA], cooking OA [COA], and biomass burning OA [BBOA]) and two SOA factors (aqueous-phase oxidized OA [aq-OOA, herein termed aqSOA] and oxygenated OA [OOA]) (Zhang et al., 2024). SOA contributed 51% of total OA mass concentrations on average, falling between previously reported summer and winter values (Duan et al., 2020; Li et al., 2023; Sun et al., 2016; W. Q. Xu et al., 2019; J. Zhao et al., 2019). The concentration of OA was predominantly governed by SOA formation under both clean ($PM_1 < 5$ μg $m^{-3}$) and high aerosol loading ($PM_1 > 30$ μg $m^{-3}$) conditions, contributing 57% and 60% of total OA, respectively. In both cases, SOA was mainly driven by OOA and aq-OOA, respectively (Figure S8 in Supporting Information S1), highlighting their dominance in photochemical and aqueous-phase chemical pathways. The mean fractional contribution of aq-OOA to total SOA was 29%, which is comparable to previously reported ratios for urban Beijing (Li et al., 2023; Ma et al., 2022; Sun et al., 2016; W. Q. Xu et al., 2019; J. Zhao et al., 2019) and closely aligns with ML-based estimates (31%). Notably, we observed a rapid increase in the aq-OOA/SOA ratio from ~4% to 70% as NR-$PM_1$ concentrations rose from <5 to >30 μg $m^{-3}$, signaling a regime shift from photochemical to aqueous-phase dominated SOA formation during pollution buildup.

These findings are consistent with the ML results identifying ALWC as the most critical factor influencing OA formation, providing mutually reinforcing evidence from both source apportionment model and data-driven approaches. The methodological convergence between PMF and ML interpretations strengthens confidence in aqueous-phase processes being the key driver of particulate pollution formation during high-pollution episodes.

The second most important feature is the aerosol surface area (Sa), which represents the reactive interface for heterogeneous and aqueous phase processes and directly governs mass transfer efficiency. Increased Sa enhances GPP of reaction intermediates, facilitating the condensation of semi-volatile and intermediate-volatility organic compounds (S/IVOCs). When particle diameter increased from 67 to 135 nm, the corresponding Sa rose from about 100 to 400 $\mu m^2$ $cm^{-3}$ based on the particle average number concentration ($7 \times 10^3$ $cm^{-3}$) during the observation period, resulting in a 3.5 μg $m^{-3}$ enhancement of the OA concentration (Figure 2d). Furthermore, elevated ALWC concurrently increases the effective surface area, thereby promoting aqueous-phase reactions. Ranking as the third most significant factor, CO serves as a tracer for VOCs emitted from fossil fuel combustion in urban areas, which also represent the primary precursor for SOA formation. The lower importance of CO relative to ALWC and Sa implies that precursor VOCs may be sufficient in supply, while the atmospheric conversion efficiency of VOCs emerges as the limiting factor in SOA formation.

$NH_3$ and $HNO_3$ rank as the 4th and 5th most significant factors influencing OA concentrations, respectively. The North China Plain is characterized by exceptionally high $NH_3$ emissions (Pan et al., 2018), creating a typical $NH_3$-rich environment. Under the $NH_3/NH_4^+$ buffering system, acidic gases ($H_2SO_4$ and $HNO_3$) are efficiently neutralized to form ammonium sulfate and ammonium nitrate (G. Zheng et al., 2020). In this study, sulfate concentrations averaged 1.9 μg $m^{-3}$, significantly lower than nitrate concentrations of 7.1 μg $m^{-3}$ even during high-$PM_{2.5}$ episodes. Ammonium nitrate exhibits deliquescence at lower RH compared to ammonium sulfate, demonstrating that nitrate plays a more substantial role than sulfate in elevating ALWC, which in turn promotes OA formation.

### 3.3. Factors Controlling pON Formation

The model results with pON as the dependent variable identified Sa as the most influential factor for pON formation, showing a positive contribution. This is consistent with established knowledge that increased Sa provides additional interfaces for condensation or heterogeneous reaction, enhancing the adsorption of gaseous precursors and subsequent reactions. In this study, the greater importance of Sa relative to ALWC suggests that pON formation was driven by heterogeneous processes, including GPP and interface reaction, in autumn Beijing.

Atmospheric ONs, existing in both gas and particle phases, primarily originate from interactions between VOCs and atmospheric oxidants (Ng et al., 2017). The OH during daytime and $NO_3$ during nighttime are the dominant oxidants for most VOC compounds; once the oxidants attack the double bond or the aromatic ring of VOCs, autoxidation can be triggered (Bianchi et al., 2019; Kiendler-Scharr et al., 2016; Nah et al., 2016). However, the high concentrations of NO in the boundary layer during the campaign terminate autoxidation and lead to the formation of compounds containing multiple nitrogen atoms. Those gas-phase ONs of varying volatility may

partition to the particle phase through GPP or multiphase oxidation processes, contributing significantly to pON formation (Gkatzelis et al., 2021; Ng et al., 2017). Previous field studies have consistently observed synchronous variations between pON and LO-OOA, suggesting that pON predominantly originates from photochemical processes (L. Xu et al., 2015). The diurnal pattern of ON during the campaign showed a nighttime peak, indicating the remarkable role of nitrate radical in ON formation (Ng et al., 2017). Extensive observational studies revealed that the relative importance of photochemical versus aqueous-phase pathways in pON production is highly sensitive to ambient environmental conditions (Bikkina et al., 2017; C. R. Chen et al., 2021; Y. L. Wang et al., 2021; W. Q. Xu et al., 2017). Besides, laboratory studies indicated that the hydrolysis of pON is also a critical factor affecting its concentration (Boyd et al., 2015; Day et al., 2022), a process which currently cannot be captured by ML methods but warrants more attention in future research.

Nitryl chloride ($ClNO_2$) emerges as the third most influential factor following Sa and ALWC. It primarily undergoes direct photolysis to generate highly reactive chlorine atoms that oxidize VOCs, accelerating $RO_2$ radical formation and subsequent ON production (Le Breton et al., 2018). The results also show that BC is far more important for pON than OA. This is possibly because OA formation in this study is primarily driven by aqueous-phase processes, which predominantly occur during periods of high aerosol loading with elevated ALWC. Furthermore, due to its hydrophobic nature, BC primarily participates in gas-particle processes by providing active sites for the formation of pON, rather than engaging in aqueous-phase processes to promote OA formation. $NH_3$ plays a substantial role beyond regulating aerosol inorganic composition and acid-base balance, potentially participating directly in ON formation mechanisms.

## 4. Discussion and Summary

OA formation involves source emissions, gas-phase oxidation of VOCs, and heterogeneous processes. Field observation alone may struggle to distinguish the relative importance of gas-phase oxidation and heterogeneous processes. This study employed an interpretable ML approach to successfully identify the relative contributions of ALWC and Sa that represent aqueous-phase processes and gas-phase transformation, respectively. The estimated contribution of aqueous-phase SOA formation to total SOA production based on this method was approximately 30%, consistent with the results from PMF source apportionment, demonstrating that interpretable ML can serve as an effective semi-quantitative tool. As an important component of OA, pON accounts for a higher proportion of OA under low PM conditions (Figure S8 in Supporting Information S1). The results of ML indicate that gas-phase oxidation processes contribute more significantly to pON than aqueous-phase processes, particularly under medium aerosol loading (Figure S12b in Supporting Information S1). It is consistent with the actual observation that high ALWC typically coincides with high aerosol loading. As ambient particulate matter pollution continues to improve, the frequency of heavy pollution events will decrease, and the importance of pON is expected to increase. Therefore, future research on pON precursors and formation mechanisms will be essential.

Rigorous validation is still required when applying this method to different regions or time periods. This is because significant spatiotemporal variations in actual atmospheric conditions, such as VOCs species, oxidant types, solar radiation, and RH, will lead to changes in SOA formation pathways. Therefore, it is necessary to extend the application of interpretable ML to field observation across more regions, enabling it to evolve into an efficient analytical tool with environmental universality for managing OA pollution (Pendergrass et al., 2025).

## Conflict of Interest

The authors declare no conflicts of interest relevant to this study.

## Data Availability Statement

The data in this manuscript are publicly available at https://doi.org/10.5281/zenodo.17221024 (Liu, 2025).

**Acknowledgments**
This work was financially supported by the National Natural Science Foundation of China (22327806, 42405098, 42205098, 42207137, and 22188102).

## References

Bianchi, F., Kurtén, T., Riva, M., Mohr, C., Rissanen, M. P., Roldin, P., et al. (2019). Highly oxygenated organic molecules (HOM) from gas-phase autoxidation involving peroxy radicals: A key contributor to atmospheric aerosol. *Chemical Reviews*, *119*(6), 3472–3509. https://doi.org/10.1021/acs.chemrev.8b00395

Bikkina, S., Kawamura, K., & Sarin, M. (2017). Secondary organic aerosol formation over coastal ocean: Inferences from atmospheric water-soluble low molecular weight organic compounds. *Environmental Science & Technology*, *51*(8), 4347–4357. https://doi.org/10.1021/acs.est.6b05986

Boyd, C. M., Sanchez, J., Xu, L., Eugene, A. J., Nah, T., Tuet, W. Y., et al. (2015). Secondary organic aerosol formation from the $\beta$-pinene+$NO_3$ system: Effect of humidity and peroxy radical fate. *Atmospheric Chemistry and Physics*, *15*(13), 7497–7522. https://doi.org/10.5194/acp-15-7497-2015

Chen, C. R., Zhang, H. X., Yan, W. J., Wu, N. A., Zhang, Q., & He, K. B. (2021). Aerosol water content enhancement leads to changes in the major formation mechanisms of nitrate and secondary organic aerosols in winter over the North China Plain. *Environmental Pollution*, *287*, 10. https://doi.org/10.1016/j.envpol.2021.117625

Chen, T. Z., Liu, J., Chu, B. W., Ge, Y. L., Zhang, P., Ma, Q. X., & He, H. (2023). Combined smog chamber/oxidation flow reactor study on aging of secondary organic aerosol from photooxidation of aromatic hydrocarbons. *Environmental Science & Technology*, *57*(37), 13937–13947. https://doi.org/10.1021/acs.est.3c04089

Chen, T. Z., Liu, J., Liu, Y., Ma, Q., Ge, Y., Zhong, C., et al. (2020). Chemical characterization of submicron aerosol in summertime Beijing: A case study in southern suburbs in 2018. *Chemosphere*, *247*, 125918. https://doi.org/10.1016/j.chemosphere.2020.125918

Day, D. A., Campuzano-Jost, P., Nault, B. A., Palm, B. B., Hu, W., Guo, H., et al. (2022). A systematic re-evaluation of methods for quantification of bulk particle-phase organic nitrates using real-time aerosol mass spectrometry. *Atmospheric Measurement Techniques*, *15*(2), 459–483. https://doi.org/10.5194/amt-15-459-2022

Denkenberger, K. A., Moffet, R. C., Holecek, J. C., Rebotier, T. P., & Prather, K. A. (2007). Real-time, single-particle measurements of oligomers in aged ambient aerosol particles. *Environmental Science & Technology*, *41*(15), 5439–5446. https://doi.org/10.1021/es070329l

DeRieux, W. S., Li, Y., Lin, P., Laskin, J., Laskin, A., Bertram, A. K., et al. (2018). Predicting the glass transition temperature and viscosity of secondary organic material using molecular composition. *Atmospheric Chemistry and Physics*, *18*(9), 6331–6351. https://doi.org/10.5194/acp-18-6331-2018

Donahue, N. M., Robinson, A. L., Stanier, C. O., & Pandis, S. N. (2006). Coupled partitioning, dilution, and chemical aging of semivolatile organics. *Environmental Science & Technology*, *40*(8), 2635–2643. https://doi.org/10.1021/es052297c

Duan, J., Huang, R. J., Li, Y., Chen, Q., Zheng, Y., Chen, Y., et al. (2020). Summertime and wintertime atmospheric processes of secondary aerosol in Beijing. *Atmospheric Chemistry and Physics*, *20*(6), 3793–3807. https://doi.org/10.5194/acp-20-3793-2020

Duan, J., Huang, R. J., Wang, Y., Xu, W., Zhong, H., Lin, C., et al. (2024). Measurement report: Size-resolved secondary organic aerosol formation modulated by aerosol water uptake in wintertime haze. *Atmospheric Chemistry and Physics*, *24*(13), 7687–7698. https://doi.org/10.5194/acp-24-7687-2024

Ervens, B., Turpin, B. J., & Weber, R. J. (2011). Secondary organic aerosol formation in cloud droplets and aqueous particles (aqSOA): A review of laboratory, field and model studies. *Atmospheric Chemistry and Physics*, *11*(21), 11069–11102. https://doi.org/10.5194/acp-11-11069-2011

Farmer, D. K., Matsunaga, A., Docherty, K. S., Surratt, J. D., Seinfeld, J. H., Ziemann, P. J., & Jimenez, J. L. (2010). Response of an aerosol mass spectrometer to organonitrates and organosulfates and implications for atmospheric chemistry. *Proceedings of the National Academy of Sciences of the United States of America*, *107*(15), 6670–6675. https://doi.org/10.1073/pnas.0912340107

Fry, J. L., Draper, D. C., Zarzana, K. J., Campuzano-Jost, P., Day, D. A., Jimenez, J. L., et al. (2013). Observations of gas- and aerosol-phase organic nitrates at BEACHON-RoMBAS 2011. *Atmospheric Chemistry and Physics*, *13*(17), 8585–8605. https://doi.org/10.5194/acp-13-8585-2013

Gao, S., Keywood, M., Ng, N. L., Surratt, J., Varutbangkul, V., Bahreini, R., et al. (2004). Low-molecular-weight and oligomeric components in secondary organic aerosol from the ozonolysis of cycloalkenes and $\alpha$-pinene. *Journal of Physical Chemistry A*, *108*(46), 10147–10164. https://doi.org/10.1021/jp047466e

Gkatzelis, G. I., Papanastasiou, D. K., Karydis, V. A., Hohaus, T., Liu, Y., Schmitt, S. H., et al. (2021). Uptake of water-soluble gas-phase oxidation products drives organic particulate pollution in Beijing. *Geophysical Research Letters*, *48*(8), 12. https://doi.org/10.1029/2020gl091351

Guo, H., Xu, L., Bougiatioti, A., Cerully, K. M., Capps, S. L., Hite, J. R., Jr., et al. (2015). Fine-particle water and pH in the southeastern United States. *Atmospheric Chemistry and Physics*, *15*(9), 5211–5228. https://doi.org/10.5194/acp-15-5211-2015

Hallquist, M., Wenger, J. C., Baltensperger, U., Rudich, Y., Simpson, D., Claeys, M., et al. (2009). The formation, properties and impact of secondary organic aerosol: Current and emerging issues. *Atmospheric Chemistry and Physics*, *9*(14), 5155–5236. https://doi.org/10.5194/acp-9-5155-2009

Hou, L. L., Dai, Q., Song, C., Liu, B., Guo, F., Dai, T., et al. (2022). Revealing drivers of haze pollution by explainable machine learning. *Environmental Science & Technology Letters*, *9*(2), 112–119. https://doi.org/10.1021/acs.estlett.1c00865

Huang, D. D., Zhang, Q., Cheung, H. H. Y., Yu, L., Zhou, S., Anastasio, C., et al. (2018). Formation and evolution of aqSOA from aqueous-phase reactions of phenolic carbonyls: Comparison between ammonium sulfate and ammonium nitrate solutions. *Environmental Science & Technology*, *52*(16), 9215–9224. https://doi.org/10.1021/acs.est.8b03441

Huang, R. J., Li, Y. J., Chen, Q., Zhang, Y., Lin, C., Chan, C. K., et al. (2025). Secondary organic aerosol in urban China: A distinct chemical regime for air pollution studies. *Science*, *389*(6763), 10. https://doi.org/10.1126/science.adq2840

Huang, W., Yang, Y., Wang, Y., Gao, W., Li, H., Zhang, Y., et al. (2021). Exploring the inorganic and organic nitrate aerosol formation regimes at a suburban site on the North China Plain. *Science of the Total Environment*, *768*, 8. https://doi.org/10.1016/j.scitotenv.2020.144538

Jia, L., & Xu, Y. F. (2014). Effects of relative humidity on ozone and secondary organic aerosol formation from the photooxidation of benzene and ethylbenzene. *Aerosol Science & Technology*, *48*(1), 1–12. https://doi.org/10.1080/02786826.2013.847269

Jimenez, J. L., Canagaratna, M. R., Donahue, N. M., Prevot, A. S. H., Zhang, Q., Kroll, J. H., et al. (2009). Evolution of organic aerosols in the atmosphere. *Science*, *326*(5959), 1525–1529. https://doi.org/10.1126/science.1180353

Kiendler-Scharr, A., Mensah, A. A., Friese, E., Topping, D., Nemitz, E., Prevot, A. S. H., et al. (2016). Ubiquity of organic nitrates from nighttime chemistry in the European submicron aerosol. *Geophysical Research Letters*, *43*(14), 7735–7744. https://doi.org/10.1002/2016gl069239

Kuang, Y., He, Y., Xu, W., Yuan, B., Zhang, G., Ma, Z., et al. (2020). Photochemical aqueous-phase reactions induce rapid daytime formation of oxygenated organic aerosol on the North China Plain. *Environmental Science & Technology*, *54*(7), 3849–3860. https://doi.org/10.1021/acs.est.9b06836

Lambe, A. T., Onasch, T. B., Massoli, P., Croasdale, D. R., Wright, J. P., Ahern, A. T., et al. (2011). Laboratory studies of the chemical composition and cloud condensation nuclei (CCN) activity of secondary organic aerosol (SOA) and oxidized primary organic aerosol (OPOA). *Atmospheric Chemistry and Physics*, *11*(17), 8913–8928. https://doi.org/10.5194/acp-11-8913-2011

Le Breton, M., Hallquist, Å. M., Pathak, R. K., Simpson, D., Wang, Y., Johansson, J., et al. (2018). Chlorine oxidation of VOCs at a semi-rural site in Beijing: Significant chlorine liberation from $ClNO_2$ and subsequent gas- and particle-phase Cl-VOC production. *Atmospheric Chemistry and Physics*, *18*(17), 13013–13030. https://doi.org/10.5194/acp-18-13013-2018

Li, Y., Lei, L., Sun, J., Gao, Y., Wang, P., Wang, S., et al. (2023). Significant reductions in secondary aerosols after the three-year action plan in Beijing summer. *Environmental Science & Technology*, *57*(42), 15945–15955. https://doi.org/10.1021/acs.est.3c02417

Lim, Y. B., Tan, Y., Perri, M. J., Seitzinger, S. P., & Turpin, B. J. (2010). Aqueous chemistry and its role in secondary organic aerosol (SOA) formation. *Atmospheric Chemistry and Physics*, *10*(21), 10521–10539. https://doi.org/10.5194/acp-10-10521-2010

Lin, C. S., Huang, R. J., Duan, J., Zhong, H. B., & Xu, W. (2021). Primary and secondary organic nitrate in Northwest China: A case study. *Environmental Science & Technology Letters*, *8*(11), 947–953. https://doi.org/10.1021/acs.estlett.1c00692

Liu, J. (2025). Data of paper: Machine learning-driven identification of factors governing secondary organic aerosol formation during autumn in Beijing [Dataset]. *Zenodo*. https://doi.org/10.5281/zenodo.17221024

Lundberg, S. M., Erion, G., Chen, H., DeGrave, A., Prutkin, J. M., Nair, B., et al. (2020). From local explanations to global understanding with explainable AI for trees. *Nature Machine Intelligence*, *2*(1), 56–67. https://doi.org/10.1038/s42256-019-0138-9

Lundberg, S. M., & Lee, S. I. (2017). A unified approach to interpreting model predictions. In *Paper presented at 31st annual conference on neural information processing systems (NIPS), neural information processing systems (Nips)*.

Ma, W., Zheng, F., Zhang, Y., Chen, X., Zhan, J., Hua, C., et al. (2022). Weakened gas-to-particle partitioning of oxygenated organic molecules in liquified aerosol particles. *Environmental Science & Technology Letters*, *9*(10), 837–843. https://doi.org/10.1021/acs.estlett.2c00556

McFiggans, G., Mentel, T. F., Wildt, J., Pullinen, I., Kang, S., Kleist, E., et al. (2019). Secondary organic aerosol reduced by mixture of atmospheric vapours. *Nature*, *565*(7741), 587–593. https://doi.org/10.1038/s41586-018-0871-y

McVay, R. C., Cappa, C. D., & Seinfeld, J. H. (2014). Vapor-wall deposition in chambers: Theoretical considerations. *Environmental Science & Technology*, *48*(17), 10251–10258. https://doi.org/10.1021/es502170j

Nah, T., Sanchez, J., Boyd, C. M., & Ng, N. L. (2016). Photochemical aging of $\alpha$-pinene and $\beta$-pinene secondary organic aerosol formed from nitrate radical oxidation. *Environmental Science & Technology*, *50*(1), 222–231. https://doi.org/10.1021/acs.est.5b04594

Ng, N. L., Brown, S. S., Archibald, A. T., Atlas, E., Cohen, R. C., Crowley, J. N., et al. (2017). Nitrate radicals and biogenic volatile organic compounds: Oxidation, mechanisms, and organic aerosol. *Atmospheric Chemistry and Physics*, *17*(3), 2103–2162. https://doi.org/10.5194/acp-17-2103-2017

Nguyen, T. K. V., Zhang, Q., Jimenez, J. L., Pike, M., & Carlton, A. G. (2016). Liquid water: Ubiquitous contributor to aerosol mass. *Environmental Science & Technology Letters*, *3*(7), 257–263. https://doi.org/10.1021/acs.estlett.6b00167

Nie, W., Yan, C., Huang, D. D., Wang, Z., Liu, Y., Qiao, X., et al. (2022). Secondary organic aerosol formed by condensing anthropogenic vapours over China's megacities. *Nature Geoscience*, *15*(4), 255–261. https://doi.org/10.1038/s41561-022-00922-5

Odum, J. R., Hoffmann, T., Bowman, F., Collins, D., Flagan, R. C., & Seinfeld, J. H. (1996). Gas/particle partitioning and secondary organic aerosol yields. *Environmental Science & Technology*, *30*(8), 2580–2585. https://doi.org/10.1021/es950943+

Pan, Y., Tian, S., Zhao, Y., Zhang, L., Zhu, X., Gao, J., et al. (2018). Identifying Ammonia hotspots in China using a national observation network. *Environmental Science & Technology*, *52*(7), 3926–3934. https://doi.org/10.1021/acs.est.7b05235

Pankow, J. F., & Bidleman, T. F. (1992). Interdependence of the slopes and intercepts from log-log correlations of measured gas-particle partitioning and vapor pressure—I. Theory and analysis of available data. *Atmospheric Environment, Part A: General Topics*, *26*(6), 1071–1080. https://doi.org/10.1016/0960-1686(92)90039-n

Pendergrass, D. C., Jacob, D. J., Oak, Y. J., Dang, R., Yang, L. H., Beaudry, E., et al. (2025). Wintertime trends of fine particulate matter (PM2.5) in South Korea, 2012-2022: Response of nitrate and organic components to decreasing $NO_x$ emissions. *Geophysical Research Letters*, *52*(19), 9. https://doi.org/10.1029/2025gl116091

Rogers, M. J., Joo, T., Hass-Mitchell, T., Canagaratna, M. R., Campuzano-Jost, P., Sueper, D., et al. (2025). Humid summers promote urban aqueous-phase production of oxygenated organic aerosol in the northeastern United States. *Geophysical Research Letters*, *52*(4), e2024GL112005. https://doi.org/10.1029/2024gl112005

Sapkota, S., Shekhar, P., Murphy, B., Pye, H. O. T., Hennigan, C. J., & El-Sayed, M. M. H. (2025). Seasonal assessment of secondary organic aerosol formed through aqueous pathways in the eastern United States. *ACS Earth and Space Chemistry*, *9*(4), 876–887. https://doi.org/10.1021/acsearthspacechem.4c00392

Sarrafzadeh, M., Wildt, J., Pullinen, I., Springer, M., Kleist, E., Tillmann, R., et al. (2016). Impact of $NO_x$ and OH on secondary organic aerosol formation from $\beta$-pinene photooxidation. *Atmospheric Chemistry and Physics*, *16*(17), 11237–11248. https://doi.org/10.5194/acp-16-11237-2016

Shiraiwa, M., & Seinfeld, J. H. (2012). Equilibration timescale of atmospheric secondary organic aerosol partitioning. *Geophysical Research Letters*, *39*(24), 6. https://doi.org/10.1029/2012gl054008

Song, M. J., Liu, P. F. F., Hanna, S. J., Zaveri, R. A., Potter, K., You, Y., et al. (2016). Relative humidity-dependent viscosity of secondary organic material from toluene photo-oxidation and possible implications for organic particulate matter over megacities. *Atmospheric Chemistry and Physics*, *16*(14), 8817–8830. https://doi.org/10.5194/acp-16-8817-2016

Sun, Y. L., Du, W., Fu, P., Wang, Q., Li, J., Ge, X., et al. (2016). Primary and secondary aerosols in Beijing in winter: Sources, variations and processes. *Atmospheric Chemistry and Physics*, *16*(13), 8309–8329. https://doi.org/10.5194/acp-16-8309-2016

Wang, Y. H., Clusius, P., Yan, C., Dällenbach, K., Yin, R., Wang, M., et al. (2022). Molecular composition of oxygenated organic molecules and their contributions to organic aerosol in Beijing. *Environmental Science & Technology*, *56*(2), 770–778. https://doi.org/10.1021/acs.est.1c05191

Wang, Y. L., Huang, D. D., Huang, W., Liu, B., Chen, Q., Huang, R., et al. (2021). Enhanced nitrite production from the aqueous photolysis of nitrate in the presence of Vanillic acid and implications for the roles of light-absorbing organics. *Environmental Science & Technology*, *55*(23), 15694–15704. https://doi.org/10.1021/acs.est.1c04642

Wu, Z., Wang, Y., Tan, T., Zhu, Y., Li, M., Shang, D., et al. (2018). Aerosol liquid water driven by anthropogenic inorganic salts: Implying its key role in haze formation over the North China Plain. *Environmental Science & Technology Letters*, *5*(3), 160–166. https://doi.org/10.1021/acs.estlett.8b00021

Xie, Y., Wang, G., Wang, X., Chen, J., Chen, Y., Tang, G., et al. (2020). Nitrate-dominated $PM_{2.5}$ and elevation of particle pH observed in urban Beijing during the winter of 2017. *Atmospheric Chemistry and Physics*, *20*(8), 5019–5033. https://doi.org/10.5194/acp-20-5019-2020

Xu, L., Kollman, M. S., Song, C., Shilling, J. E., & Ng, N. L. (2014). Effects of $NO_x$ on the volatility of secondary organic aerosol from isoprene photooxidation. *Environmental Science & Technology*, *48*(4), 2253–2262. https://doi.org/10.1021/es404842g

Xu, L., Suresh, S., Guo, H., Weber, R. J., & Ng, N. L. (2015). Aerosol characterization over the southeastern United States using high-resolution aerosol mass spectrometry: Spatial and seasonal variation of aerosol composition and sources with a focus on organic nitrates. *Atmospheric Chemistry and Physics*, *15*(13), 7307–7336. https://doi.org/10.5194/acp-15-7307-2015

Xu, W. Q., Han, T., Du, W., Wang, Q., Chen, C., Zhao, J., et al. (2017). Effects of aqueous-phase and photochemical processing on secondary organic aerosol formation and evolution in Beijing, China. *Environmental Science & Technology*, *51*(2), 762–770. https://doi.org/10.1021/acs.est.6b04498

Xu, W. Q., Sun, Y., Wang, Q., Zhao, J., Wang, J., Ge, X., et al. (2019). Changes in aerosol chemistry from 2014 to 2016 in winter in Beijing: Insights from high-resolution aerosol mass spectrometry. *Journal of Geophysical Research: Atmospheres*, *124*(2), 1132–1147. https://doi.org/10.1029/2018jd029245

Xuan, H. Y., Liu, J., Zhao, Y., Cao, Q., Chen, T., Wang, Y., et al. (2024). Relative humidity driven nocturnal HONO formation mechanism in autumn haze events of Beijing. *npj Climate and Atmospheric Science*, *7*(1), 193. https://doi.org/10.1038/s41612-024-00745-8

Yang, C., Yao, N., Xu, L., Chen, G., Wang, Y., Fan, X., et al. (2023). Molecular composition of anthropogenic oxygenated organic molecules and their contribution to organic aerosol in a coastal city. *Environmental Science & Technology*, *57*(42), 15956–15967. https://doi.org/10.1021/acs.est.3c03244

Yang, Y., Huang, L. B., Zhao, M., Wu, Y., Xu, Y. H., Li, Q. Y., et al. (2025). Multiphase reactions of organic peroxides and nitrite as a source of atmospheric organic nitrates. *Nature Communications*, *16*(1), 8. https://doi.org/10.1038/s41467-025-60696-3

Zare, A., Romer, P. S., Nguyen, T., Keutsch, F. N., Skog, K., & Cohen, R. C. (2018). A comprehensive organic nitrate chemistry: Insights into the lifetime of atmospheric organic nitrates. *Atmospheric Chemistry and Physics*, *18*(20), 15419–15436. https://doi.org/10.5194/acp-18-15419-2018

Zhang, C. Y., Wang, Y. H., Liu, J., Chen, T. Z., Huang, W., Liu, Z. R., et al. (2024). Insight into wet scavenging effects on sulfur and nitrogen containing organic compounds in urban Beijing. *npj Climate and Atmospheric Science*, *7*(1), 205. https://doi.org/10.1038/s41612-024-00756-5

Zhao, J., Qiu, Y., Zhou, W., Xu, W., Wang, J., Zhang, Y., et al. (2019). Organic aerosol processing during winter severe haze episodes in Beijing. *Journal of Geophysical Research: Atmospheres*, *124*(17–18), 10248–10263. https://doi.org/10.1029/2019jd030832

Zhao, X., Wang, Q., Zhang, P., Wang, Y., Li, S., Su, Z., et al. (2025). Surface uptake of exogenous volatile organic compounds enhances the $NO_2$-to-HONO conversion on soot. *ACS ES&T Air*, *2*(6), 1107–1114. https://doi.org/10.1021/acsestair.5c00072

Zheng, G., Su, H., Wang, S., Andreae, M. O., Poschl, U., & Cheng, Y. (2020). Multiphase buffer theory explains contrasts in atmospheric aerosol acidity. *Science*, *369*(6509), 1374–1377. https://doi.org/10.1126/science.aba3719

Zheng, Y., Chen, Q., Cheng, X., Mohr, C., Cai, J., Huang, W., et al. (2021). Precursors and pathways leading to enhanced secondary organic aerosol formation during severe haze episodes. *Environmental Science & Technology*, *55*(23), 15680–15693. https://doi.org/10.1021/acs.est.1c04255